Mengzeng CHENG[1], Xu CAI[1,2], Guoxiang WU[1]

Key Laboratory of Control of Power Transmission and Transformation (KLCPTT), Wind Power Research Centre (WPRC), School of Electronic Information and Electrical Engineering, Shanghai Jiao Tong University (1)
State Key Laboratory of Ocean Engineering, School of Naval Architecture, Ocean and Civil Engineering, Shanghai Jiao Tong University (2)

Investigation of Transient Torque during a Power System Fault in Wind Power Turbines Having a DFIG and Crowbar Circuit

Abstract. *To study the influence of power system voltage drop on the doubly-fed induction generator (DIFG) shaft, this paper analyzes the electromagnetic torque change of the DFIG through approximated analytical expression of the stator fault current and rotor fault current obtained by the superposition between transient current based on vector method and steady-state current based on equivalent circuit method, and then the DFIG torque change situations under the following circumstances: the three-phase symmetrical voltage dip of stator terminal, the converter of the rotor side is cut off, and the crowbar circuit is put into the operation, will be analyzed through the method. Furthermore, on the basis of theoretical analysis, a 2MW DFIG model is established by PSCAD, and the simulation results validate that the torque changes of the DFIG shaft could be analyzed by the expression of the DFIG torque during the grid voltage drops through the superposition of the transient current and steady-state current. At last, the optimizing value of the crowbar resistance is given.*

Streszczenie. *W artykule analizuje się zmiany momentu elektromagnetycznego podwójnie zasilanego generator indukcyjnego DFIG poprzez ocenę prądów wirnika i stojana otrzymaną przez superpozycję prądów przejściowych (metoda wektorowa) i prądu stanu ustalonego (metoda obwodów zastępczych). Badania symulacyjne potwierdziły słuszność metody. (**Badania momentu przejściowego podczas zakłóceń pracy systemu z turbiną wiatrową wyposażoną w układ DFIG**)*

Keywords: Voltage dip, Doubly-fed Induction Generator (DIFG), Electromagnetic Torque, Crowbar Circuit, Shaft.
Słowa kluczowe: zapad napięcia, DFIG, moment elektromagnetyczny.

Introduction

In China and other parts of the world, most wind farms are located in the regions that have rich wind resource, however, because these regions are remote and in bad conditions, the power system connected with the wind farms is far away from load centers and weak [1]. This kind of weak grid experiences various disturbances, for example the frequent faults voltage dip and voltage unbalance. And the operation of wind turbines is impacted significantly by the grid during the faults [2]. In the past, wind turbines were disconnected from the grid after a grid fault occurs. However, according to the recent grid code updates, it is now necessary that wind turbines remain connected to the grid within a certain voltage range for a given time duration[3]. The different grid codes of several countries depend on their system characteristics and operation standards. For example, according to the new E.on (German electric utility) grid code of 2006, wind farms should support the power system and restore grid voltage quickly by generating reactive current during a grid fault [4].

Among the varieties of variable speed wind turbines which are installed in large wind farms, the doubly fed induction generator (DFIG) is the most widely used [5]. But as far as achieving low voltage ride-through (LVRT) is concerned, the most challenging one is the DFIG due to its unique structure. The stator terminals of a DFIG are directly connected to the grid with a power electronic converter connected between the rotor windings of the DFIG and the grid. However, wind turbines based on the DFIG are very sensitive to grid disturbances, especially voltage dips. During a fault, the transient currents on the stator are large and oscillatory, which can be reflected on the rotor windings. The high currents can cause thermal breakdown of the converter [6].

When there is a large grid voltage dip, in order to limit the surge current as well as protect the rotor side converter, a DFIG equipped with a crowbar circuit is becoming more popular and reliable method today in achieving LVRT [7,8,9]. But Crowbar technology will have the following problems: on the one hand, the method employs a crowbar circuit connected to the rotor windings, which is equivalent that the rotor side is connected with a DFIG with a large resistor, and converting the DFIG to an asynchronous induction generator that will consume more reactive power and possibly result in voltage instability, which doesn't assist in voltage recovery of the grid. On the other hand, when the crowbar circuit is cut in or off, the large transient current could cause a large electromagnetic oscillation to the DFIG [10]. In addition, when the DFIG is under sub-synchronous operation and the crowbar circuit is cut into the operation, there is an opposing torque, but after a few hundred milliseconds, when the crowbar circuit is cut off, there is a reverse change again in the torque. So, the oscillatory electromagnetic torque and average torque with varying direction appear on the DFIG shaft. And because the mechanical torque and electromagnetic torque do not match frequently, the torsional stress of oscillatory torque is loaded on the shaft system resulting in the large mechanical stress of the DFIG, which could cause a fatal destruction on the DFIG shaft system [11]. In paper [12], it is shown that the gearbox is a troublesome component within the wind power turbine. For a typical turbine, 20% of the downtime is due to gearbox failures, and an average gearbox failure takes about 256h to repair. This pays a very high price for the system operation and failure maintenances.

In this paper, a two-mass model is created for the shaft of wind power system. First, the DFIG transient current generated from the voltage drop is obtained by the vector method, and the steady-state current generated by the residual voltage is calculated through the steady-state equivalent circuit method. Second, the stator fault current and rotor fault current are obtained by the superposition between the transient current and the steady-state current, and then the DFIG torque changes are calculated at the time of the grid voltage drops. Additionally, the expression of DFIG torque changes during a grid fault based on the superposition method is a kind of approximate analytical expression, but the error does not affect the quantitative analysis of the DFIG. This calculation method is simple and easily analyzed and understood. This paper analyzes the influence of the crowbar circuit on the DFIG shaft during the grid fault, which is estimated through the transient electromagnetic torque and mechanical torque of the DFIG at a certain wind speed.

The model of DFIG systems

The aerodynamic model of a DFIG

Wind generator converts the mechanical energy of wind turbines into the electrical energy, while the wind turbines' mechanical torque and mechanical energy always vary with the changes of the wind speed. According to Betz's law, the mechanical energy and mechanical torque can be calculated as follows [13]:

$$P_m = \frac{1}{2}\rho A C_p V^3 \tag{1}$$

$$T_m = \frac{P_m}{\omega_t} = \frac{1}{2}\rho A C_P \frac{R}{\lambda} V^2 \tag{2}$$

where: ρ – air density (Kg/m3), V – wind speed (m/s), A – turbine swept area (m2), C_p – wind turbine's power coefficient, R – blade radius (m), ω_t – turbine's angular velocity (rad/s), and $\lambda=\omega_t*R/V$ is the tip speed ratio.

The shaft model

Under steady state operating conditions, the mechanical and electrical decoupling can be achieved through the decoupling control of the variable speed wind turbines, and the torsional vibration is basically filtered by the converter. However, for the serious power system fault such as a three-phase short circuit fault, the fault could cause the voltage drops at the DFIG stator terminal, so the oscillations of the DFIG electromagnetic torque will occur, and then the oscillations of the shaft are correspondingly shown.

In the transient stability studies, in order to reflect correctly the response characteristics of wind turbine at the time of the large disturbances in the power system, the two-mass shaft system model are required. Among the two masses, one represents the inertia of wind turbine, and the other represents the generator inertia, and additionally, the wind turbine and generator are connected through the gearbox. The mathematical equation of the two-mass model [14,15] can be expressed as:

$$\begin{cases} 2H_T \dfrac{d\omega_T}{dt} = T_T - T_M - D_T\omega_T \\ 2H_M \dfrac{d\omega_M}{dt} = T_M - T_E - D_M\omega_M \\ \dfrac{d\theta_s}{dt} = \omega_1\left(\omega_T - \omega_M\right) \\ T_M = K_s \cdot \theta_s - D_s\left(\omega_M - \omega_T\right) \end{cases} \tag{3}$$

where: H_T – wind turbine inertia, H_M – generator inertia, K_S – stiffness coefficient of the shaft, DT, DM and DS are the damping coefficient of the wind turbine rotor, generator rotor and shaft respectively, θ_S – relative angular displacement between the two masses, T_T, T_M and T_E are the mechanical torque of the wind turbine, the mechanical torque of the generator rotor and the electromagnetic torque of the generator respectively, ω_T – speed of the wind turbine, ω_M – speed of the generator rotor, ω_1 – synchronous speed. The shaft model of the wind turbine is shown in Figure 1.

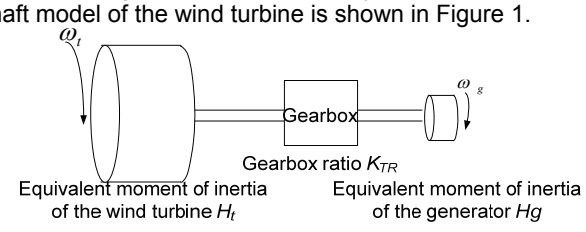

Fig.1. The diagram of two-mass shaft mode of the wind turbine

The DFIG model

This section determines the response of DFIG to a symmetrical voltage drops at its stator terminals. For the analysis, a space vector description is used. In a rotating reference frame, the equivalent circuit of the DFIG could be described by:

$$U_s = R_s I_s + j\omega\psi_s + \frac{d}{dt}\psi_s \tag{4}$$

$$U_r = R_r I_r + j(\omega - \omega_r)\psi_r + \frac{d}{dt}\psi_r \tag{5}$$

$$\psi_s = L_s I_s + L_m I_r \tag{6}$$

$$\psi_r = L_r I_r + L_m I_s \tag{7}$$

where: R –resistance, U – voltage, I – current, ψ–flux linkage, ω – arbitrary speed. The subscripts s and r denote stator and rotor quantities respectively. L_s, L_r and L_m are the stator equivalent self-inductance, the rotor equivalent self-inductance and the mutual inductance respectively. In these equations, all parameters are converted into the stator side. Based on these equations, the equivalent circuit of the DFIG that is shown in Fig. 2 can be obtained. It can be used for transient analysis of the DFIG.

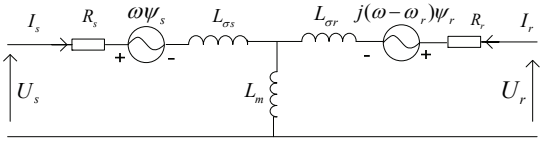

Fig.2 Equivalent circuit of the DFIG in an arbitrary rotating reference frame

The relationship between electromagnetic torque T_E, mechanical angular velocity Ω_r and mechanical power P_m requires the following:

$$T_E = \frac{P_m}{\Omega_r} = \frac{\mathrm{Re}(-j\omega_r\psi_r I_r^*)}{\Omega_r} = -p_n\psi_r \times I_r \tag{8}$$

As can be seen from the above equation, the electromagnetic torque is proportional to the vector product of the rotor flux and rotor current. The following expression is obtained by substituting the equation (7) into the equation (8),

$$\begin{aligned} T_E &= -p_n\left(L_r I_r + L_m I_s\right)\times I_r \\ &= -p_n L_m I_s \times I_r \\ &= p_n L_m I_r \times I_s \\ &= p_n L_m \,\mathrm{Im}\left(I_s I_r^*\right) \end{aligned} \tag{9}$$

Additionally, there are no restrictions about the stator voltage, rotor voltage and current waveforms in the transient torque expression.

The theoretical analysis of transient electromagnetic torque of DFIG with a Crowbar circuit

The crowbar is cut in and the RSC is effectively removed from the DFIG. In this condition, the DFIG behaves as an induction machine which has a rotor with large resistance or inductance. DFIG with the crowbar operation is shown in Figure 3.

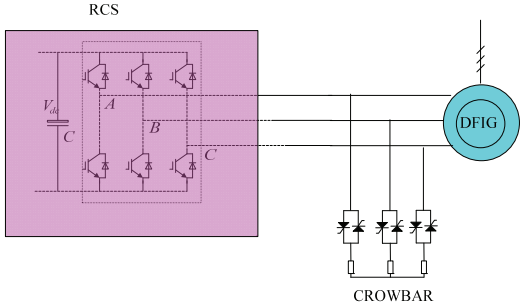

Fig.3. The operation diagram of DFIG with a crowbar circuit

According to the literature [16], under steady state operating conditions, there are $\frac{d}{dt}\psi_s = 0$ and $\frac{d}{dt}\psi_r = 0$ in the synchronous rotating reference frame. If the stator resistance R_s is neglected, the expression for the stator voltage and rotor voltage can be obtained from (4)-(7):

(10) $$U_s \approx j\omega_s \psi_s$$

(11) $$U_r \approx js\omega_s \psi_r$$

and,

(12) $$U_s = s \cdot U_r$$

The DFIG is under normal operating conditions before the grid fault, and the voltage space vector of the stator rotates at the synchronous speed of ω_s with a constant amplitude V. The voltage vector at the stator terminal can be expressed as:

(13) $$U_s = V_s \cdot e^{j\omega_s t}$$

The expression of the stator flux can be obtained from (4) and (13):

(14) $$\psi_s = \frac{V_s}{j\omega_s} \cdot e^{j\omega_s t}$$

The generator is assumed to be operating under normal conditions when, at a given moment in time t_0, a three-phase voltage dip occurs to the grid at $t=t_0$, and a voltage dip of depth (or profundity) p occurs at $t \geq t_0$:

(15) $$U_s = \begin{cases} V_s e^{j\omega_s t} & t < t_0 \\ (1-p) V_s e^{j\omega_s t} & t \geq t_0 \quad (0 \leq p \leq 1) \end{cases}$$

From the magnetic flux conservation principle, the stator flux and rotor flux remain the same as their pre-fault steady-state values after the grid fault occurs, setting V_s and V_r as the stator and rotor voltage amplitude value of the pre-fault steady-state condition. After the grid fault, in stationary reference frame, the initial value of stator flux generated by the voltage drop can be expressed:

(16) $$\psi_{s0} = \frac{pV_s}{j\omega_s}$$

Considering the demagnetizing effect of the stator DC components, in the stationary reference frame, the initial value of rotor flux is:

(17) $$\psi_{r0} = \frac{pV_r}{js\omega_s} \cdot e^{j\omega_r t} = \frac{pV_s}{j\omega_s} \cdot e^{j\omega_r t}$$

where: ω_t – electrical angular velocity of the rotor corresponding to the mechanical angular velocity.

From the equation (16) and (17), it can be seen that the amplitude values of ψ_s and ψ_r are approximately equal. After the crowbar is switched on, the DFIG transient current could be analyzed by the principle of asynchronous induction motor. And the DFIG flux transient component is generated by the drop voltage. In reality, the space vector rotates slowly and is damped exponentially. The space vector rotates faster for a larger stator and rotor resistance. The time constant for the damping of the DC components in stator and rotor are given by [10]:

(18) $$T_s = \sigma \frac{L_s}{R_s}$$

(19) $$T_r = \sigma \frac{L_r}{R_r}$$

And the leakage factor

(20) $$\sigma = 1 - \frac{L_m^2}{L_s L_r}$$

The transient currents of the stator and rotor under the grid fault state can be obtained from the flux, substituting the equations (16) and (17) into (6) and (7),

(21) $$I_{ls}(t) = \frac{pV_s}{j\sigma L_s \omega_s} \left(e^{-t/T_s} - \frac{L_m}{L_r} \cdot e^{-t/T_r} \cdot e^{j\omega_r t} \right)$$

(22) $$I_{lr}(t) = \frac{pV_s}{j\sigma L_r \omega_s} \left(e^{-t/T_r} \cdot e^{j\omega_r t} - \frac{L_m}{L_s} \cdot e^{-t/T_s} \right)$$

The equations (21) and (22) are the analytical expressions of the transient current components of the DFIG stator and rotor in the stationary reference frame. This expression shows that the stator and rotor currents consist of two terms, determined by the stator and rotor damping time constant, and a term with a constant angle caused by the natural flux.

Residual voltage of the power grid makes the DFIG operate under the steady-state condition. The equivalent circuit of the DFIG with a crowbar circuit under the steady-state operation is shown in Figure 4.

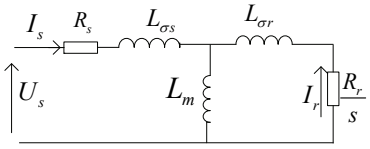

Fig.4 The equivalent circuit of DFIG with a crowbar circuit under the steady-state operation

In order to simplify the calculations, some parameters which have little effect on the results could be considered negligible, and these parameters are: 1) space and time harmonics, 2) magnetic saturation, 3) iron loss, 4) the stator equivalent resistance. Ignoring the above parameters, the input impedance of the stator terminal is:

(23) $$Z_s = j\omega_s L_{\sigma s} + \frac{j\omega_s L_m \left(j\omega_s L_{\sigma r} + \frac{R_r}{s} \right)}{j\omega_s L_r + \frac{R_r}{s}}$$

In the stationary reference frame of the stator, through the equivalent circuit shown in Figure 4, the steady-state current expression of the stator is as follows:

(24) $$I_{ss}(t) = \frac{(1-p)V_s}{Z_s} \cdot e^{j\omega_s t}$$

, and the steady-state current expression of the DFIG rotor is:

(25) $$I_s(t) = I_{ss}(t) + I_{ls}(t) = \frac{(1-P)V_s}{Z_s} \cdot e^{j\omega_s t} + \frac{pV_s}{j\sigma L_s \omega_s} \left(e^{-t/T_s} - \frac{L_m}{L_r} \cdot e^{-t/T_r} \cdot e^{j\omega_r t} \right)$$

According to the superposition theorem, in the voltage drop, the stator current expression of the DFIG with a crowbar circuit is:

(26) Similarly, the rotor current expression is:

(27) $$I_r(t) = I_{rs}(t) + I_{lr}(t) = -\frac{j\omega L_m}{j\omega L_r + \frac{R_r}{s}} \cdot \frac{(1-P)V_s}{Z_s} \cdot e^{j\omega_s t} + \frac{pV_s}{j\sigma L_r \omega_s} \left(e^{-t/T_r} \cdot e^{j\omega_r t} - \frac{L_m}{L_s} \cdot e^{-t/T_s} \right)$$

Substituting the equations (26) and (27) into (9), the expression of electromagnetic torque changes of the DFIG with a crowbar circuit during the voltage drop is as follows: (28)

$$T_E = p_n L_m \operatorname{Im}\left(I_s(t) I_r(t)^*\right) = \frac{p_n V_s^2 \frac{R_r}{s}}{\omega_s\left[\left(\frac{R_r}{s}\right)^2 + \omega_s^2\left(L_{\sigma s} + L_{\sigma r}\right)^2\right]}\{-(1-p)^2$$

$$+ p(1-p) X_m\left[\left(\frac{1}{X_r^{'}} - \frac{1}{X_s^{'}}\right) e^{j\omega_r t} e^{-t/T_r} + \left(\frac{1}{X_s^{'}} - \frac{1}{X_r^{'}}\right) e^{-t/T_s}\right] \cos \omega_s t$$

$$+ p(1-p)[\frac{X_m\left(X_{\sigma s} + X_{\sigma r}\right)}{\frac{R_r}{s}}\left[\left(\frac{1}{X_r^{'}} - \frac{1}{X_s^{'}}\right) e^{j\omega_r t} e^{-t/T_r} + \left(\frac{1}{X_s^{'}} - \frac{1}{X_r^{'}}\right) e^{-t/T_s}\right]$$

$$+ \frac{R_r}{s}\left(\frac{1}{X_r^{'}} e^{j\omega_r t} e^{-t/T_r} - \frac{1}{X_r^{'}} e^{-t/T_s}\right)]\sin \omega_s t\}$$

where: $X_s^{'} = \omega_s\left(L_s - \frac{L_m^2}{L_r}\right)$, $X_r^{'} = \omega_s\left(L_r - \frac{L_m^2}{L_s}\right)$.

From the equation (28), it could be seen that the oscillatory electromagnetic torque generated from the voltage drop consists of the following components: 1) the steady-state component of torque, 2) the torque generated by the interaction between the steady-state AC current components of the stator and rotor and the DC attenuation parts of the stator and rotor, which is the pulsating torque with a slow attenuation, 3) the torque generated by the interaction between the decaying DC components of the stator and rotor, which is the torque component with a fast attenuation and could be considered negligible. So when the voltage drop occurs on the stator side of the DFIG, the electromagnetic torque consists of not only the steady-state components, but also the attenuation parts, and additionally, this is a complex process.

Simulation Results and Analysis

In order to verify that the proposed analytical method could be used to analyze the electromagnetic torque changes of the DFIG with a crowbar circuit under the fault condition, a model was established by using PSCAD/EMTDC software, and simulations were carried out for a 2MW DFIG (please refer to the Appendix) connected to the power system bus. The transformer is rated at 2.5MVA and is conceived to step up a voltage of 690V to a grid voltage of 10kV. When the simulation is performed for a voltage dip of 80% starting at t=3s and with a duration of 0.5s, block the converter pulse on the rotor side and switch on the crowbar circuit (the crowbar resistances are different). And the transient comparative results about the electromagnetic torque, speed and the torsional stress of shaft are shown in Figure 5, presented in per-unit value.

In Figure 5, the voltage of the DFIG stator terminal is shown in Figure (a), and the corresponding comparison result of the DFIG electromagnetic torques with different crowbar resistors is presented in Figure (b). From the comparison result, it can be seen that when the DFIG is connected with the crowbar circuit resistance of 0 Ω, the oscillation of the electromagnetic torque is the fiercest with the oscillation amplitude change from -2.8 (p.u.) to 2.0 (p.u.) in the first cycle and the maximum change of 4.8 (p.u.). But when the DFIG is connected with the crowbar circuit resistances of 0.3Ω and 0.5Ω respectively, their corresponding maximum peak values of the oscillation amplitude of the electromagnetic torque are -1.5 (p.u.) and -1.2 (p.u.). Therefore, from the simulation results, the electromagnetic torque consists of the transient components and the steady-state components, furthermore, the decay rate of the steady-state torque and transient torque at a certain speed can be altered by the crowbar resistance. And the bigger the crowbar circuit resistance is, the better the suppression of the DFIG transient torque is, but when the crowbar resistance is beyond a certain value, the attenuation of the DFIG torque is not obvious. From the equation (28) in the third section, it could be seen that the steady-state torque and transient attenuation torque are all related to the DFIG terminal voltage and the resistances of crowbar circuit connected with the rotor terminal. And the bigger the crowbar circuit resistance is, the faster the torque decays and the smaller the torque below and above the synchronous speed is. So, the simulation results agree with the theoretical analysis of the third section.

(a) Voltage of the DFIG stator terminal

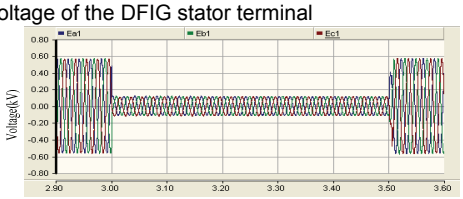

(b) Electromagnetic torque

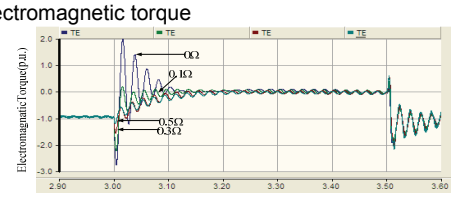

(c) DFIG speed

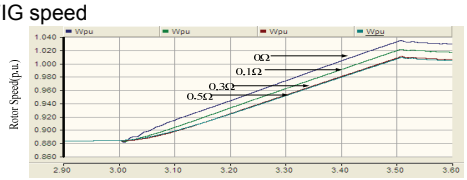

(d) Mechanical torque

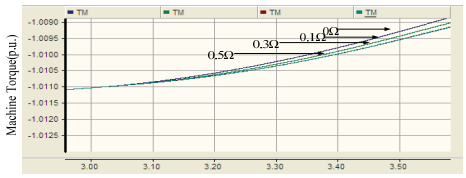

(e) Sum of electromagnetic torque and mechanical torque

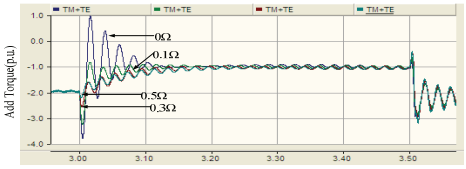

Fig.5 Torque and speed changes of the DFIG with different crowbar circuits during the grid voltage dip of 80%

Figure (c) shows the changes of the DFIG speed, and the smaller the crowbar circuit resistance is, the faster the DFIG speed increases. In the 0.5s duration of the power grid fault, when the DFIG is connected with the crowbar circuit resistance of 0 Ω, the DFIG speed increases fastest with the change of 0.15 (p.u.). But when the DFIG is connected with the crowbar circuit resistances of 0.3Ω and 0.5Ω respectively, their corresponding changes of the DFIG speed are almost the same with the change of 0.12 (p.u.). Figure (d) shows the corresponding changes of the mechanical torque with different crowbar circuit resistances. And because the largest change value is 0.0016 (p.u.), the mechanical torque is almost constant. Furthermore, in the steady-state operation of the DFIG, because the electromagnetic torque and mechanical torque are equal

and opposite in directions, the torque on the DFIG shaft is the sum of these two parts. Since the direction of generator model is positive with the reference direction of electrical motor in PSCAD, the torque of the DFIG is negative in the power generation state. In addition, because the mechanical torque is almost constant, the DFIG electromagnetic torque is almost the sum torque. Therefore, from Figure (e) simulation result, the change process of the electromagnetic torque is almost the same to Figure (b)'s, but the mechanical torque is superimposed in the values.

When there is a voltage drop of 80%, the electromagnetic torque changes of the DFIG with a crowbar circuit under the super-synchronous condition and sub-synchronous condition are presented respectively in Figure 6, and A represents the super-synchronous state, B is on behalf of the sub-synchronous state. Figure (b) shows the electromagnetic torque changes of the DFIG with a Crowbar circuit under the above conditions, and Figure (c) presents the changes about the sum of the electromagnetic torque and mechanical torque of the DFIG with a Crowbar circuit. When the grid voltage drops, for both the state A and B, the transient decay components play a major role in the electromagnetic torque changes, while the steady-state components don't, and this is due to the big voltage dips and could be seen from the equation (28) in the theoretical analysis. In addition, when the grid voltage is restored, the electromagnetic torque will reach to -3.2 (p.u.) under the super-synchronous condition, while the electromagnetic torque reaches only to -1.8 (p.u.) under the sub-synchronous condition, and the reason is that the power generated by the DFIG in the super-synchronous state is greater than it in the sub-synchronous state and the current overshoot in the grid voltage recovery under the super-synchronous condition is greater than it under the sub-synchronous condition, then it lead that the electromagnetic torque oscillation in the super-synchronous state is also greater than the electromagnetic torque oscillation in the sub-synchronous.

(a) Voltage of the DFIG stator terminal

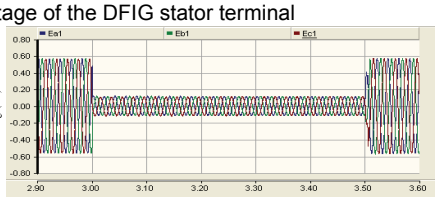

(b) Electromagnetic torque

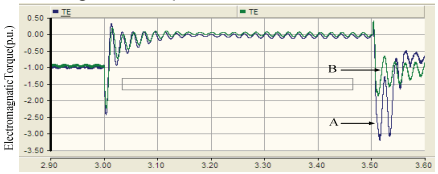

(c) Sum of the electromagnetic torque and the mechanical torque

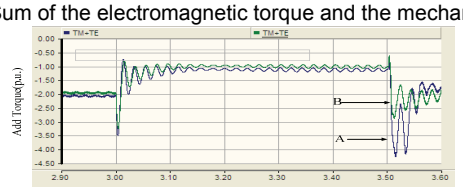

(d) DFIG speed

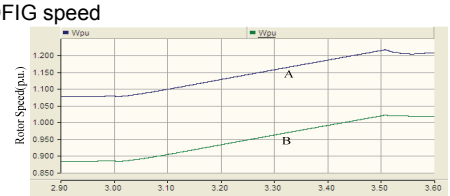

Fig.6 Torque and speed changes of the DFIG with a crowbar circuit under the super-synchronous and sub-synchronous conditions during the grid voltage dip of 80%

Compared with Figure 6, Figure 7 shows the electromagnetic torque changes under the same conditions as the Figure 6's except of the grid voltage of 50%, and Figure 7 aims to present the influence of voltage drop amplitude on the shaft torque. Figure (a) shows the amplitude of the voltage drop. As compared with Figure 6 (b), the steady-state components play a major role in the DFIG torque, which is due to a high voltage of the DFIG stator terminal. In the first cycle, the maximum change of the transient torque 2.3(p.u.), and the average electromagnetic torque acts in the opposite direction to the pre-fault torque under the sub-synchronous condition. And Figure (d) shows that the DFIG speed increases by 0.11(p.u.) in the super-synchronous state and the DFIG speed increases by 0.15(p.u.) in the sub-synchronous state. So, the average electromagnetic torque is rated to the voltage drop amplitude, which agrees with the equation (28) in the theoretical analysis.

(a) Voltage of the DFIG stator terminal

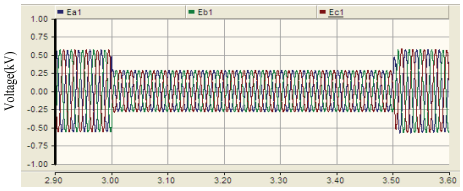

(b) Electromagnetic torque

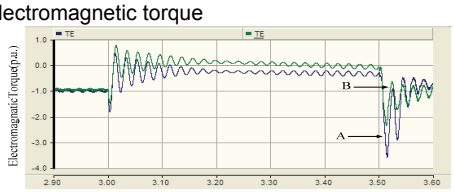

(c) Sum of the electromagnetic torque and the mechanical torque

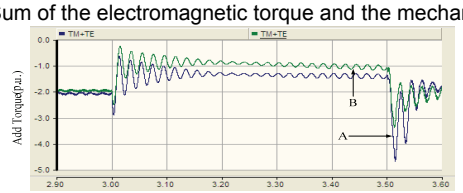

(d) DFIG speed

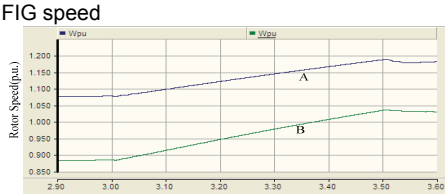

Fig.7 Torque and speed changes of the DFIG with a crowbar circuit under the super-synchronous and sub-synchronous conditions during the grid voltage dip of 50%

Conclusion

The paper uses the method combining the vector method and the steady-state equivalent circuit method to analyze the electromagnetic torque expression of the DFIG with a crowbar circuit during the grid voltage drops. Although there are some errors in the electromagnetic torque expression through the method, they do not affect the quantitative analysis of the DFIG and the conclusions. From the theoretical analysis, it can be seen that when the grid voltage drops, the DFIG electromagnetic torque consists of two parts that the steady-state and transient components, and the electromagnetic torque value is determined by the DFIG terminal voltage, the crowbar resistance and the DFIG speed.

The simulation results of electromagnetic torque changes are consistent with the theoretical analysis, and the larger the crowbar resistance is, the better the inhibition effect on the transient electromagnetic torque is. When the crowbar resistance increases to a certain value, the impact

on the DFIG shaft is not obvious, and viewed from the effect on the shaft of 2MW DFIG, the crowbar circuit resistances of 0.3Ω-0.5Ω is appropriate.

There is a required additional remark that resistance reaching to a certain value will make the voltage of the DFIG rotor side too high and increase the reactive power absorption, which isn't discussed in this paper and await further researches. However, the method presented in the paper will be useful to calculate the crowbar circuit of the DFIG with different capacity levels to obtain an appropriate crowbar circuit resistance, which could decrease the impact on the shaft of wind turbine.

Acknowledgments: This work was supported by Shanghai Science and Technology Commission (No. 08DZ1200504 and No. 09DZ1201303), Key Laboratory Fund (No. AE010803) and Natural Science Foundation of Jiangsu Higher Education Institutions (10KJD480004).

Appendix

2MW DFIG EQUIVALENT CIRCUIT PARAMETERS:
Model base values: Sbase=2.0 MW, fbase = 50 Hz, Vbase= 690 V (rms line–line)
Winding connection (stator/rotor): Y-Y
Turns ratio: $N_s/N_r = 0.45$
Stator resistance: R_s=0.00488p.u.
Stator leakage inductance: $L_{\sigma s}$=0.1386p.u.
Rotor resistance: R_r=0.00549 p.u.
Rotor leakage inductance: $L_{\sigma r}$=0.1493p.u.
Magnetizing inductance: L_m=3.9527p.u.
H=3.5s.

REFERENCES

[1] R. Piwko, N. Miller, J. Sanchez-Gasca, X. Yuan, R. Dai, J. Lyons, Integrating Large Wind Farms into Weak Power Grids with Long Transmission Lines*, The 5th IEEE Power Electronics and Motion Control Conference IPEMC 2006,* Aug 14-16, 2006, Shanghai, China.

[2] M. R. Rathi, N. Mohan, A Novel Robust Low Voltage and Fault Ride Through For Wind Turbine Application Operating in Weak Grids. *The 31st Annual Conference of IEEE Industrial Electronics Society IECON 2005,* Nov 6-10, 2005, Raleigh, NC, USA.

[3] I. Erlich, U. Bachmann, Grid Code Requirements Concerning Connection and Operation of Wind Turbines in Germany, *IEEE Power Engineering Society General Meeting 2005,* June 12-16, 2005, Washington D.C., USA.

[4] M. Tsili, C. Patsiouras, S. Papathanassiou, Grid Code Requirements for Large Wind Farms: A Review of Technical Regulations and Available Wind Turbine Technologies, *European Wind Energy Conference & Exhibition EWEC 2008,* Mar 31-Apr 3, 2008, Brussels, Belgium.

[5] J. Morren, Haan de, S.W.H., Ridethrough of Wind Turbines with Doubly-fed Induction Generator during a Voltage Dip, *IEEE Transactions on Energy Conversion, vol. 20 n. 2,* June 2005, pp. 435-441.

[6] D. Xiang, R. Li, P. J. Tavner, S. Yang, Control of a Doubly Fed Induction Generator in a Wind Turbine during Grid Fault Ride-through, *IEEE Transaction on Energy Conversion, vol. 21 n. 3,* September 2006, pp.652-662.

[7] R. Lohde, S. Jensen, A. Knop, F. W. Fuchs, Analysis of Three Phase Grid Failure and Doubly Fed Induction Generator Ride-through Using Crowbars, *European Conference on Power Electronics and Applications 2007,* Sept 2-5, 2007, Aalborg, Denmark.

[8] D. H. Anca, M. Gabriele, Fault Ride-through Capability of DFIG Wind Turbines, *Renewable Energy, vol. 32*, July2007, pp. 1594-1610.

[9] W. Zhang, P. Zhou., Y. He, Analysis of the By-pass Resistance of an Active Crowbar for Doubly-fed Induction Generator Based Wind Turbines under Grid Faults, *International Conference on Electrical Machines and Systems ICEMS 2008*, Oct 17-20, 2008, Wuhan, China.

[10] J. Morren, Haan de, S.W.H., Short-Circuit Current of Wind Turbines with Doubly Fed Induction Generator, *IEEE Transaction on Energy Conversion, vol. 22 n. 1,* March 2007, pp. 174-180 .

[11] C. Jauch, J. Matevosyan, T. Ackermann, S. Bolik, International Comparison of Requirements for Connection of Wind Turbines to Power Systems. *Wind Energy, vol. 8,* August 2005, pp. 295-306.

[12] J. Ribrant, L.M. Bertling. Survey of Failures in Wind Power Systems with Focus on Swedish Wind Power Plants during 1997-2005, *IEEE Transaction on Energy Conversion, vol. 22 n. 1,* March 2007, pp. 167-173.

[13] F. Yu, Q. Liu, J. Zhang Flexible Grid-connection Technique and Novel Maximum Wind Power Tracking Algorithm for Doubly-Fed Wind Power Generator, *The 33rd Annual Conference of the IEEE on Industrial Electronics Society IECON 2007,* Nov 5-8, 2007, Taipei, Taiwan.

[14] V. Akhmatov, *Analysis of Dynamic Behavior of Electric Power Systems with Large Amount of Wind Power,* Ph.D. dissertation, Technical University of Denmark, Copenhagen, Denmark, 2003.

[15] M.A. Poller, Doubly-fed Induction Machine Models for Stability Assessment of Wind Farms, *IEEE Power Tech Conference Proceedings 2003*, June 23-26, 2003, Bologna, Italy.

[16] J. Yao, Y. Liao, Analysis on the Operation of an AC Excited Wind Energy Conversion System with Crowbar Protection, *Automation of Electric Power Systems, vol. 31 n. 23,* 2007, pp. 79-83.

***Authors**: Mengzeng Cheng, a Ph.D. student in electric power system and automation at Shanghai Jiaotong University, Room No. B107, Ruth Mulan Chu Chao Building, Min Hang Campus of Shanghai Jiao Tong University, No.800 Dongchuan Road, Min Hang, Shanghai, 200240, E-mail：chengmengzeng@126.com*
Xu Cai, a professor, doctor tutor and the director of Wind Power Research Center of Shanghai Jiao Tong University.
Guoxiang Wu, a postdoctor in the wind power research center of Shanghai Jiao Tong University.